KEK_J-PARC-PAC2012-XV

Letter of Intent for J-PARC 50 GeV Proton Synchrotron

γ-ray spectroscopy of a well deformed *sd*-shell nucleus: $^{25}_{\Lambda}$Mg

T. Koike*, N. Chiga, K. Hagino, F. Hiruma, R. Honda, K. Hosomi, Y. Matsumoto, K. Miwa, A. Sasaki, H. Tamura, Y. Tanimura, M. Ukai, and T. O. Yamamoto

Department of Physics, Tohoku University, Sendai, 980-8578, Japan

K. Shirotori

Research Center for Nuclear Physics, Ibaraki, Osaka, 567-0047, Japan

M. Isaka and M. Kimura

Department of Physics, Graduate School of Science,

Hokkaido University, Sapporo, 060-0810, Japan

Abstract

A γ-ray spectroscopy of $^{25}_{\Lambda}$Mg is proposed using a natural magnesium target. The excited states of the hypernucleus will be populated following the (K^-,π^-) reaction provided by the K1.1 or K1.8 beam line at J-PARC with the K^- momentum of 0.9 GeV/c and 1.8 GeV/c, respectively. The SKS system and the Hyperball-J Ge array will be used. The core nucleus, ^{24}Mg is one of the most deformed nucleus among the *sd*-shell nuclei with a suspected triaxial quadrupole deformation. The results of the recent calculations on $^{25}_{\Lambda}$Mg are summarized. The yield estimate and the results of simulations are given.

PACS numbers: 21.80.+a,23.20.Lv,21.60.Gx,27.20.+n

* tkoike@lambda.phys.tohoku.ac.jp

I. INTRODUCTION

Many atomic nuclei are known to posses stable non-spherical mass distributions or said to be deformed in their ground states. The onset of nuclear deformation is evidenced, most notably, by observations of non-zero quadrapole moment and/or so called rotational spectra of which excitation energy is expressed as

$$E_x = \frac{I(I+1)\hbar^2}{2J}, \tag{1}$$

where E_x, I, and J are an excitation energy, a total angular momentum, and a moment of inertia, respectively. The relationship between the deformation and the rotational spectra is that of spontaneous breaking of rotational symmetry by a nucleus and an elementary collective rotation (Nambu-Goldstone mode) in which a total angular momentum is shared among the constituent nucleons. Therefore, a response of nuclear shape to an external stimulus will be mirrored in the elementary rotational mode. It is of an unique and interesting theme to investigate a nuclear shape by looking at a dynamical response of nuclei as a whole to an addition of Λ hyperon with a strangeness. More pictorially, an impurity Λ is dropped in a nuclear vacuum (a ground state). Experimentally, modern hypernuclear γ-ray spectroscopy with Germanium detector arrays have achieved sensitivity to resolve these excitation modes[1].

Up to now, γ-ray spectroscopy of p-shell hypernuclei has been carried out systematically, while that of sd-shell region awaits for the E13 experiment at J-PARC and this letter of intent, which are expected to be followed by other proposals in the future. One of the major findings of the investigation was an observation of shrinkage of the core nucleus, ^{6}Li, of $^7_\Lambda$Li[2]. From the life time measurement of the $5/2^+$ excited state in $^7_\Lambda$Li, extracted was an absolute B($E2(5/2^+ \to 1/2^+)$) value which is reduced compared to that of the core nucleus. Then it was deduced that an addition of Λ in the $0s$ orbit acted effectively as glue to contract the size of the core nucleus by 19% in terms of α-deuteron intercluster distance, as predicted by Motoba, Bandō, and Ikeda[3]. Cluster model calculations of $^9_\Lambda$Be also predict a reduction of di-α cluster distance and thus reduction of the B($E2$) values[3]. Figure 1 shows the ground states and the first member states of the rotational band of three well deformed p-shell nuclei, namely ^{6}Li, ^{8}Be, and ^{12}C, together with those of corresponding Λ hypernuclei. Note that 3^+ in ^{6}Li, 0^+ and 2^+ in ^{8}Be are unbound while their Λ spin doublet states are bound in $^7_\Lambda$Li and $^9_\Lambda$Be. The numbers in the figure are the excitation energies in

MeV. For the hypernuclei, spin averaged values are shown. A notable feature is that the core nuclei respond differently to the addition of Λ. A more surprising and perplexing aspect is that a reduction and almost no change in the excitation energy is observed in ${}^{7}_{\Lambda}$Li and ${}^{9}_{\Lambda}$Be, respectively, for which the shrinkage of their di-intercluster distances are confirmed /predicted. Naively speaking, one would expect a reduction in their moment of inertia in Eq.1 and thus the rotational excitation energy to increase.

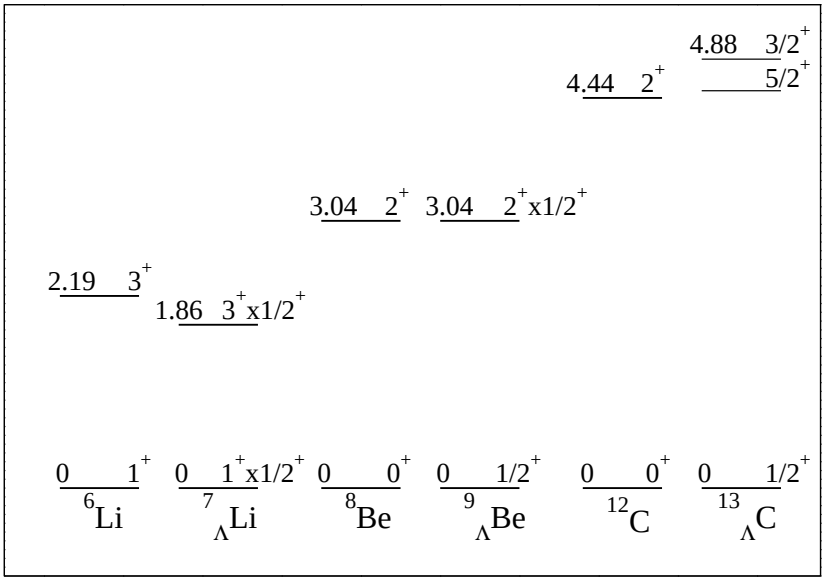

FIG. 1: The experimental low-lying spectra for ^{6}Li, ${}^{7}_{\Lambda}$Li, ^{8}Be, ${}^{9}_{\Lambda}$Be, ^{12}C, and ${}^{13}_{\Lambda}$C nuclei. The energies are denoted in the units of MeV. The energies for the $1^{+}\otimes 1/2^{+}$ and $2^{+}\otimes 1/2^{+}$ levels of the ${}^{7}_{\Lambda}$Li nucleus are obtained by spin-averaging the observed level energies for the $1/2^{+}$ (0 MeV) and the $3/2^{+}$ (0.069 MeV) states, and the $5/2^{+}$ (2.05 MeV) and the $7/2^{+}$ (2.52 MeV) states[7], respectively. The energy for the $2^{+}\otimes 1/2^{+}$ level of the ${}^{9}_{\Lambda}$Be is the spin averaged energy between the $5/2^{+}$ (3.02 MeV) and $3/2^{+}$ (3.06 MeV) states [8]. In the ${}^{13}_{\Lambda}$C nucleus, only the energy for the $3/2^{+}$ state has been measured [9], while the energy for the $5/2^{+}$ state is expected to be lower than the energy of the $3/2^{+}$ state by at most 0.36 MeV [10].

Recently a possible interpretation has been provided by employing two-body d-${}^{5}_{\Lambda}$He and α-${}^{5}_{\Lambda}$He cluster models for the ${}^{7}_{\Lambda}$Li and ${}^{9}_{\Lambda}$Be hypernuclei, respectively[4]. The results showed that a Gaussian-like interaction between two clusters leads to a stabilization of the spectrum against an addition of a Λ hyperon despite the reduction in the intercluster distance. In the case of ${}^{7}_{\Lambda}$Li, lowering of the excitation energy for the ${}^{6}\mathrm{Li}(3^{+})\otimes\Lambda(1/2^{+})$ levels can be

accounted for by considering the spin-orbit interaction between the intercluster motion and the deuteron spin; this is because the shrinkage effect increases the overlap between the wave function and the spin-orbit potential. Unlike ^{6}Li and ^{8}Be, the relatively heavier ^{12}C takes a mean field character with a sizable deformation. The presence of Λ drives its shape into a sphere and thus toward the smaller deformation[6]. The spin averaged $^{12}\mathrm{C}(2^{+}) \otimes \Lambda(1/2^{+})$ level lies higher than that of ^{12}C even if the unobserved doublet spacing is overestimated. These studies in the p-shell Λ hypernuclei demonstrate a potential of this line of research, which has not yet been actively pursued.

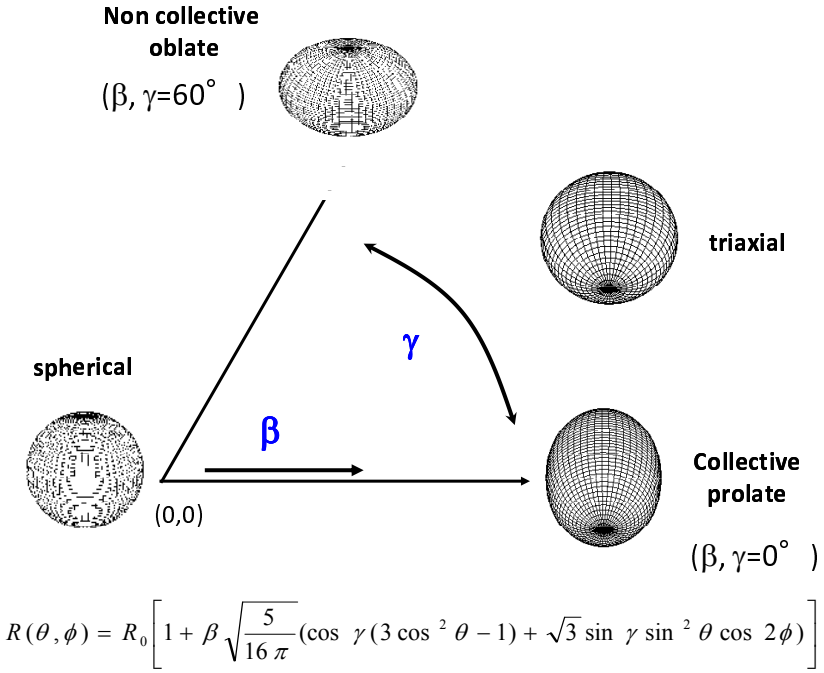

FIG. 2: Parametrization of a nuclear surface for a quadrupole deformation using β and γ. A distance to the nuclear surface from a nuclear center, $R(\theta,\phi)$, is given in the equation. All possible spheroidal shapes correspond to a polar coordinate in the (β, γ) plane between γ=0° and γ=60° where at the former and the latter γ values the spheroid has a symmetry axis and are commonly refereed to as a prolate and oblate shape, respectively. In the vast region of anywhere in between these two extremes in the deformation plane, lies a region of triaxial shape. At γ=30°, triaxiality is maximum meaning that the ratios between the long, intermediate, and short principal axis are the largest.

II. A SURVEY OF *sd*-SHELL NUCLEI AND PHYSICS OF $^{25}_{\Lambda}$MG

A. A survey of *sd*-shell nuclei

In *sd*-shell region, an island of deformation centered around Mg isotopes exists. In speaking of nuclear deformation, there have been a numerous cases of nuclei with axial deformation. Two extreme quadrupole deformations are a prolate (football-like) and an oblate (pancake) shape as illustrated in Fig. 2. In the heavier mass regions, several nuclei having an axially symmetric octupole deformation (western pear-like) have also been found[5], though the present study is limited to the quadrupole deformation. On the contrary, an experimental verification for the existence of a non-axial deformation or triaxiality has been a long debated subject despite its importance in nuclear structure studies. A triaxially deformed nucleus can rotate around the axis which does not coincide with any principal axes, having sizable components of a total angular momentum along all three principal axes, i.e. 3-D rotation of a quantum object. A sign of triaxial deformation is a low-lying second 2^+ state. Assuming a rigid triaxial shape for an even-even nucleus, Davydov and Filippov have shown that

$$\frac{E(2_2^+)}{E(2_1^+)} = \frac{1+\sqrt{1+8/9\sin^2(3\gamma)}}{1-\sqrt{1+8/9\sin^2(3\gamma)}}, \tag{2}$$

where $E(2_1^+)$ and $E(2_2^+)$ are the first and second 2^+ level energy, respectively[11]. For the most pronounced triaxiality of $\gamma = 30°$, this ratio becomes 2. As in Figure 5, this ratio for ^{24}Mg gives γ=22° and the $E(4_1^+)$, and $E(2_1^+)$ ratio is 3.0, which is close to the value of 3.3 for an ideal rotor.

B. A hypernucleus with a well deformed even-even core: $^{25}_{\Lambda}$Mg

Already a few calculations were performed on $^{25}_{\Lambda}$Mg. The first calculation for including the non-axial γ degree of freedom was carried out based on Skyrme Hartree-Fock + BCS method[12]. Potential energy surface in the (β, γ) plane was obtained for both ^{24}Mg and $^{25}_{\Lambda}$Mg to be compared. It then indicated that an addition of Λ brings the core nuclear shape toward smaller β deformation via a path in the (β, γ) deformation plane rather than along the β axis. A drastic change in shape is absent, though the softening of the potential surface

along the γ direction is visible. Since the model is based on the intrinsic reference frame where the rotational invariance is broken, the results cannot be compared directly to the experimental observation. Soon after its publication, Yao *et. al.* employed the results of Ref.[12] for input parameters for their five-dimensional collective Hamiltonian which includes quadrupole vibrational and rotational degree of freedom[13]. In this model, restoration of broken symmetries and fluctuations of collective variables are taken account. The calculated energy spectrum of the ground state rotational band resulted in a slight increase ($\sim$ 7%) of the 2_1^+ energy in ${}^{25}_{\Lambda}$Mg compared to ^{24}Mg as well as in the reduction of the B($E2 : 2_1^+ \rightarrow 0_1^+$) value by $\sim$9 %. The reduction of the B($E2$) value, though not as large as in the light cluster nuclei, is attributed to the change in deformation rather than that in the size, i.e. RMS radius, of the core nucleus, which has a different origin from the ${}^{6}_{\Lambda}$Li case.

Recently, HyperAMD (antisymmetrized molecular dynamics) with GCM (Generator Coordinate Method) were applied to calculate low-lying energy levels and B($E2$) of ${}^{25}_{\Lambda}$Mg[14], namely Λ in $0s$ orbit, as well as to those in ^{24}Mg. Figure 3 shows the calculated level schemes. The calculated density distributions of the intrinsic wave functions which have dominant contributions to the 2_1^+ and 2_2^+ states in ^{24}Mg indeed show a triaxial distribution. Not only the same applies to the $3/2_2^+$ state in ${}^{25}_{\Lambda}$Mg, but the distribution of a wave function of Λ is also triaxial suggesting that the Λ orbit is not a pure $0s$ with an admixture of non-zero angular momentum components. The calculated density distributions are shown in Fig. 4. The calculations predict a systematic displacement of the entire $K^{\pi}=2^+$ band with respect to the $K^{\pi}=0^+$ band by an increase of ΔE=200 keV, which can certainly be resolved by γ-ray spectroscopy. In contrast, relative energies within the respective band members remain unchanged.

III. EXPERIMENTAL CONSIDERATIONS

A. Objectives of γ-ray spectroscopy of ${}^{25}_{\Lambda}$Mg

- Construction of a level scheme for ${}^{25}_{\Lambda}$Mg at least up to the first 4^+ and second 2^+ state.
- Measurement of spin-doublet energy spacing of the first and the second excited states, 2_1^+ and 2_2^+, which gives a Λ spin-orbit interaction strength S_{Λ} in a *sd*-shell Λ hypernucleus.

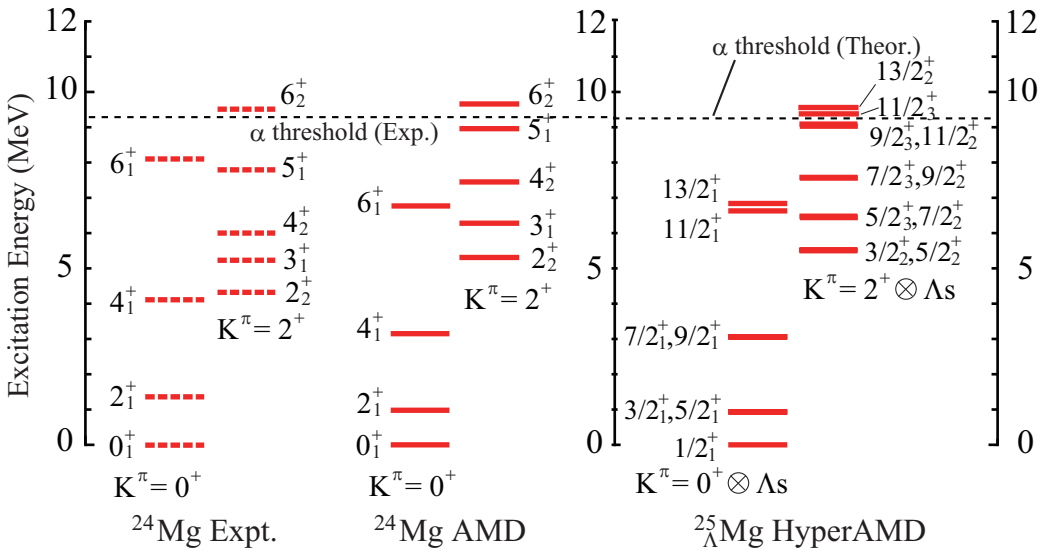

FIG. 3: Energy level schemes calculated by HyperAMD[14].(Left) Experimental and calculated level schemes of ^{24}Mg. (Right) A predicted level scheme of $^{25}_{\Lambda}$Mg where a Λ is in s orbit.

- Measurement of spin averaged 2^+_1 and 2^+_2, which gives the strength of S_N in *sd*-shell.
- The difference between the core 2^+_1 and 2^+_2 states and spin averaged 2^+_1 and 2^+_2 gives information on the change of collectivity, especially of triaxiality.
- Observation of a $0p_\Lambda \rightarrow 0s_\Lambda$ inter-shell transition with a possibility of p_Λ bound state.

B. Use of a natural target with $\gamma\gamma$ coincidence technique

One of the difficulties of γ-ray spectroscopy of hypernuclei lies in the fact that a use of an isotopically enriched target is not practical due to its extreme thickness required by the weak intensity of secondary hadron beams. Because of this constraint, the number of available targets for the experiments using the (K^-, π^-) and (π^+, K^+) reactions is severely limited to isotopes with a natural abundance of nearly 100 %. The case in point is especially relevant to an analysis of a γ-ray spectrum in singles mode. However, if the $\gamma\gamma$ coincidence analysis with enough statistics can be realized, use of a natural target containing a few isotopes is not a forbidding choice. In fact, in *sd*-shell the most abundant Mg and Cl isotopes are less then 80 %, while in *f*-shell there are three elements as such. Beyond the *f*-shell, these elements become dominant with only a few elements of a nearly 100 % abundant isotope. Therefore,

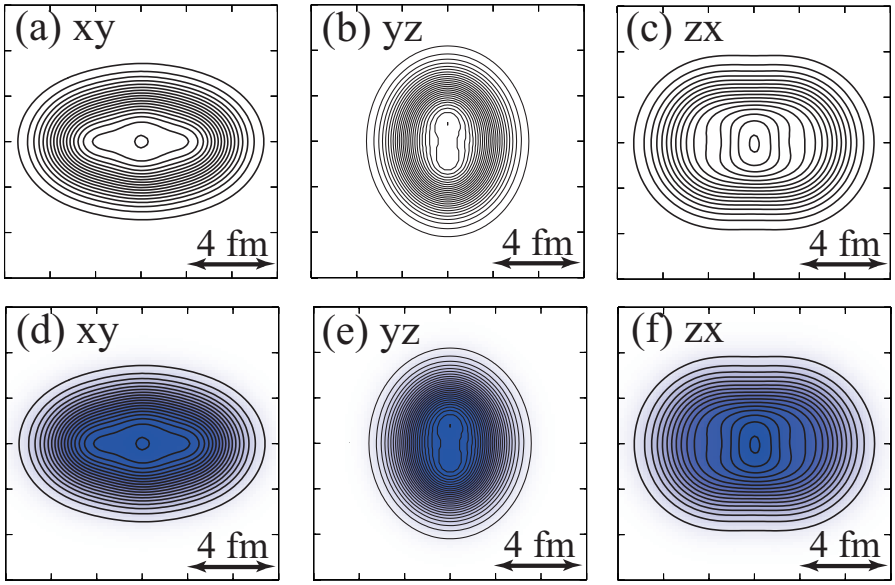

FIG. 4: (Top) Density distributions of the intrinsic wave functions, plotted in different planes, that are the main components of the 2_1^+ and 2_2^+ states of ^{24}Mg. (Bottom) The corresponding plots for the $3/2_1^+$ and $3/2_2^+$ in $^{25}_{\Lambda}$Mg. Density distributions of the nucleus and the Λ hyperon are represented by solid lines and colored region.

in the present experiment a feasibility of the proposed method will be tested using a natural Mg target combined with Hyperball-J and an intense K^- beam provided by the K1.8 or K1.1 beam line at J-PARC.

Table I lists a composition of a natural Mg target. The most abundant Mg isotope is ^{24}Mg with roughly 80 %, while less abundant ^{25,26}Mg are sharing the rest almost equally with 10 % each. Directly produced hypernuclei are $^{24,25,26}_{\Lambda}$Mg, and γ rays from these hypernuclei can be identified by gating on the bound region in the missing mass spectrum. On the other hands, those γ rays associated with hyper fragments which are produced from the excited states of $^{24,25,26}_{\Lambda}$Mg can be identified by gating on the particle unbound region of the missing mass spectrum. In Table I, also listed are expected hyper fragments following a decay above the lowest particle threshold energy. Notably, ^{25}Mg has a ground state spin of $5/2^+$ and thus is advantageous to populate high spin states in $^{25}_{\Lambda}$Mg. Moreover, $^{25}_{\Lambda}$Mg is also produced as a hyper fragment of $^{26}_{\Lambda}$Mg following a neutron emission.

Kaon momentum, p_{K^-}, of 1.8 GeV/c or 0.9 GeV/c will be suited because of its selectivity in populating non-spin-flip states and of the large elementary cross section for producing Λ.

Target	g.s. spin	$d_n \rightarrow s_\Lambda$	Hyper fragment
^{24}Mg	0^+	$^{24}_{\Lambda}$Mg (^{23}Mg)	$^{23}_{\Lambda}$Na (^{22}Na)
(0.79)			p (7.6 MeV)
^{25}Mg	$5/2^+$	$^{25}_{\Lambda}$Mg (^{24}Mg)	$^{21}_{\Lambda}$Ne (^{20}Ne)
(0.10)			α (9.3 MeV)
^{26}Mg	0^+	$^{26}_{\Lambda}$Mg (^{25}Mg)	$^{25}_{\Lambda}$Mg (^{24}Mg)
(0.11)			n (7.3 MeV)

TABLE I: Natural Mg target compositions and hypernuclei expected to be produced. The $d_n \rightarrow s_\Lambda$ column lists those produced directly in a bound region in the missing mass spectrum where a Λ occupies the lowest s orbit. Nucleus in parentheses is a corresponding core nucleus. A hyper fragment associated with a decay channel with the lowest particle threshold is listed with an emitted particle and the threshold excitation energy.

Reaction	(K^-, π^-)	
Target	natural Mg	
γ-ray detector	Hyperball-J (a full configuration of 32 Ge detectors)	
Efficiency for single γ	5.3 % at 1 MeV and 2.5 % at 3 MeV	
Efficiency for $\gamma\gamma$ coincidence	0.13 % at 1 MeV $\cap$ 3 Mev	
Ge live time	0.7	
Beam line	K1.8	K1.1
K^- momentum	1.8GeV/c	0.9 GeV/c
Downstream spectrometer	SKS	SKS
Coverage	$\pm$ 20° (horizontal), $\pm$ 5° (vertical)	$\pm$ 20° (horizontal), $\pm$ 5° (vertical)
Acceptance	100 % at 5°, 30 % at 10°	100 % at 5°, 40 % at 10°

TABLE II: Experimental conditions for the proposed experiment.

C. Yield estimate

The proposed experiment will be possibly carried out at either at the K1.8 or K1.1 beam line provided that the SKS dipole magnet and Hyperball-J will be employed. Experimental

isotopes	abundance	target	hypernucleus	N_γ/μb/h	N_γ/μb/d	$N_{\gamma\gamma}/\mu$b/d
^{24}Mg	0.79	3.40X10^{23}	$^{24}_{\Lambda}$Mg	0.5	11	0.3
^{25}Mg	0.10	4.31X10^{22}	$^{25}_{\Lambda}$Mg	0.06	1.4	0.03
^{26}Mg	0.11	4.74X10^{22}	$^{26}_{\Lambda}$Mg	0.06	1.5	0.04

TABLE III: An yield estimate for the photo peak counts N_γ and $N_{\gamma\gamma}$ of γ and $\gamma\gamma$ coincidence events, respectively, for the following conditions: (1) a natural magnesium target with a thickness of 17.38 g/cm^2 or 10cm, (2) 100k/spill K^- beam intensity, and (3) an uniform 1 μb cross section for each energy level. For the $\gamma\gamma$ coincidence estimate, a coincidence of 1 MeV and 3 MeV γ-ray energies are assumed, which approximates the transition energies of $E_\gamma(2_1^+ \rightarrow 0^+)$ and $E_\gamma(4_1^+ \rightarrow 2_1^+)$ or $E_\gamma(2_2^+ \rightarrow 2_1^+)$ in ^{24}Mg.

conditions are summarized in Table II.The SKS detection efficiency and the DAQ live time of 0.6 and 0.7, respectively, are assumed. For the photo peak detection efficiency of Hyperball-J for γ ray of various energy is simulated for a full configuration of the array with 32 Ge detectors installed. The result of the simulation is shown in Fig.6. γ rays are uniformly generated over a magnesium target of 6 cm X 1.5 cm X 10 cm dimension. The simulation accuracy for a stand alone Ge detector with a ^{60}Co point source is checked with an actual measurement. The ratio of the measured efficiency over the simulated value is around 0.9, and this is taken into account in the efficiency curve of Fig.6. With many uncertainties yet to be determined, a yield estimation for a number of photo peak counts for the γ and $\gamma\gamma$ events is listed in TableIII in unit of per 100k K^-/spill per 10cm of natural Magnesium target thickness per 1 μb cross section of each energy level.

D. Results of a simulation

A simulation for the experimental conditions of Hyperball-J and a magnesium target assumed in the yield estimation is performed. One million events are generated. Each event consists of one of a few sets of γ-ray cascades from a particular core nucleus, namely one of ^{23,24,25}Mg. The ratios among the three Mg isotopes are those of the natural abundance. Non-spin-flip doublet partners of the hypernuclear state, of which spin is related to that of the ground state of the target via either ΔL=2 or ΔL=0, are assumed to be directly

populated by the (K^-, π^-) reaction. Furthermore, the cross sections of each considered levels in $^{24,25}_{\Lambda}$Mg are weighted equally. For instance, for $^{25}_{\Lambda}$Mg, the γ cascades of (997keV, 2869keV, 1369keV), (2869keV, 1369keV), (2754keV,1369keV), and 1369keV are generated accordingly based on the level scheme of ^{24}Mg in Fig. 5. For $^{26}_{\Lambda}$Mg, seven γ transitions are generated in each event because of its complex decay paths, which should be improved in the future simulations. Doppler effects are yet to be taken into account as well. The results of the current simulation are presented in Fig. 7 and 8. As a crude estimate of the Compton suppression scheme and the background reduction, an effectiveness of PWO suppressors surrounding the Ge detectors are simulated as well, of which results are shown in red lines in Fig.7.

[1] H. Tamura *et al.*, Phys. Rev. Lett. **84**, 5963 (2000).

[2] K. Tanida *et al.*, Phys. Rev. Lett. **86**, 1982 (2001).

[3] T. Motoba, H. Band$\bar{\text{o}}$ and K. Ikeda, Prog. Theor. Phys. **80**, 189 (1983).

[4] T. K. Hagino and T. Koike, Phys. Rev. C **84** 064325 (2011).

[5] P. A. Butler and W. Nazarewicz, Rev. Mod. Phys. **68** 349 (1996).

[6] M.T. Win and K. Hagino, Phys. Rev. C **78**, 054311 (2008).

[7] M. Ukai *et al.*, Phys. Rev. C**73**, 012501(R) (2006).

[8] H. Akikawa *et al.*, Phys. Rev. Lett. **88**, 082501 (2002).

[9] H. Kohri *et al.*, Phys. Rev. C**65**, 034607 (2002).

[10] E. Hiyama, M. Kamimura, T. Motoba, T. Yamada, and Y. Yamamoto, Phys. Rev. Lett. **85**, 270 (2000).

[11] A. Davydov and F. Filippov, Nucl. Phys. **8**, 237 (1958).

[12] M.T. Win, K. Hagino, and T. Koike, Phys. Rev. C**83**, 014301 (2011).

[13] J.M. Yao, Z.P. Li, K. Hagino, M.T. Win, Y. Zhang, and J. Meng, Nucl. Phys. **A868-869**, 12 (2011).

[14] Masahiro Isaka, Hiroaki Homma, Masaaki Kimura, Akinobu Dote, and Akira Ohnish, Phys. Rev. C 85, 034303 (2012).

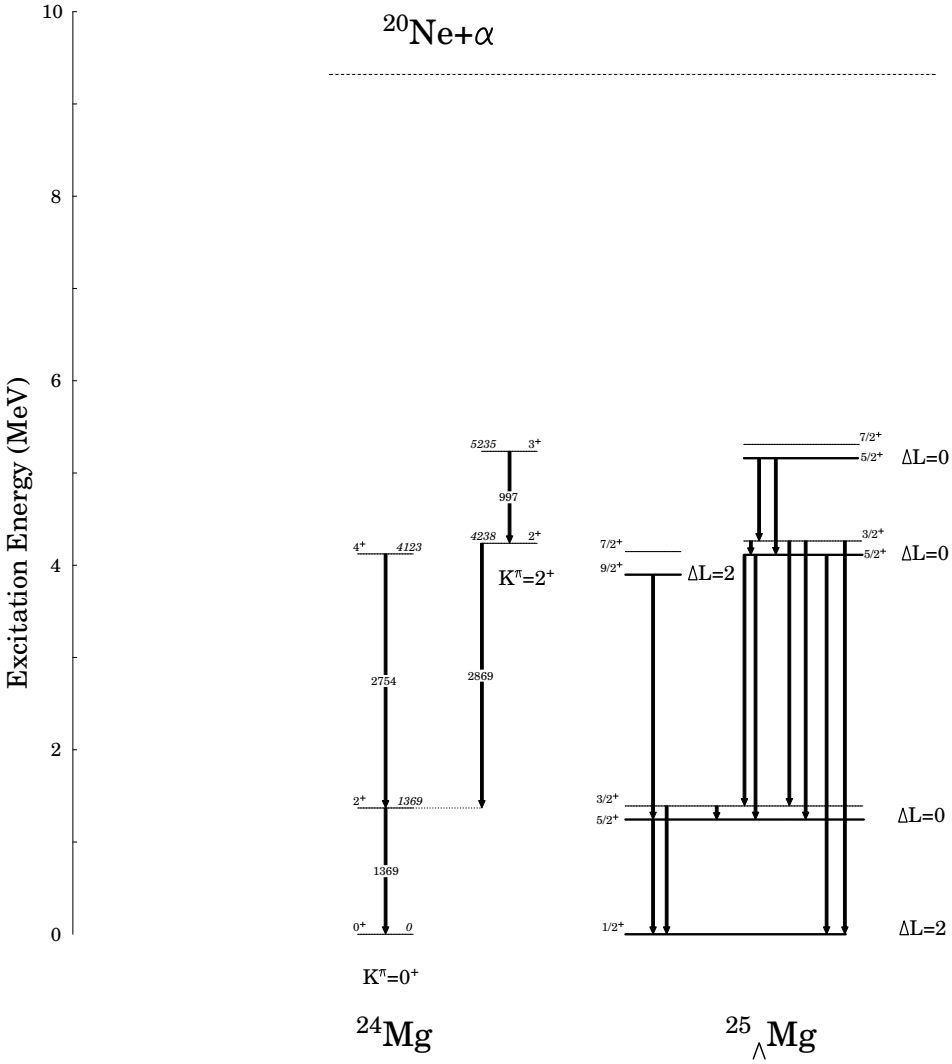

FIG. 5: Level schemes for ^{24}Mg (experimental) and $^{25}_{\Lambda}$Mg (schematic). The ground state rotational band and the γ band are labeled as $K^\pi=0^+$ and $K^\pi=2^+$, respectively. The lowest decay channel threshold corresponding to ^{20}Ne + α is at 9.3 MeV and indicated by a dotted line. Thick levels are non-spin-flip states that can be directly populated.

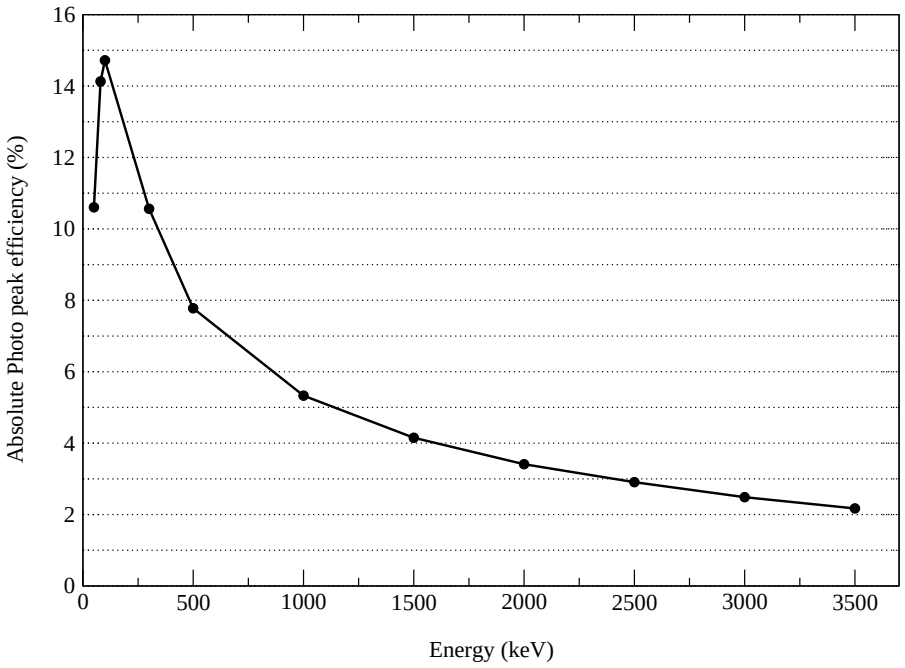

FIG. 6: Simulated Hyperball-J total photo peak efficiencies (%). γ rays are generated uniformly over a natural magnesium target of a 6 cm x1.5 cm x10 cm dimension. Adding back procedures are not taken into account.

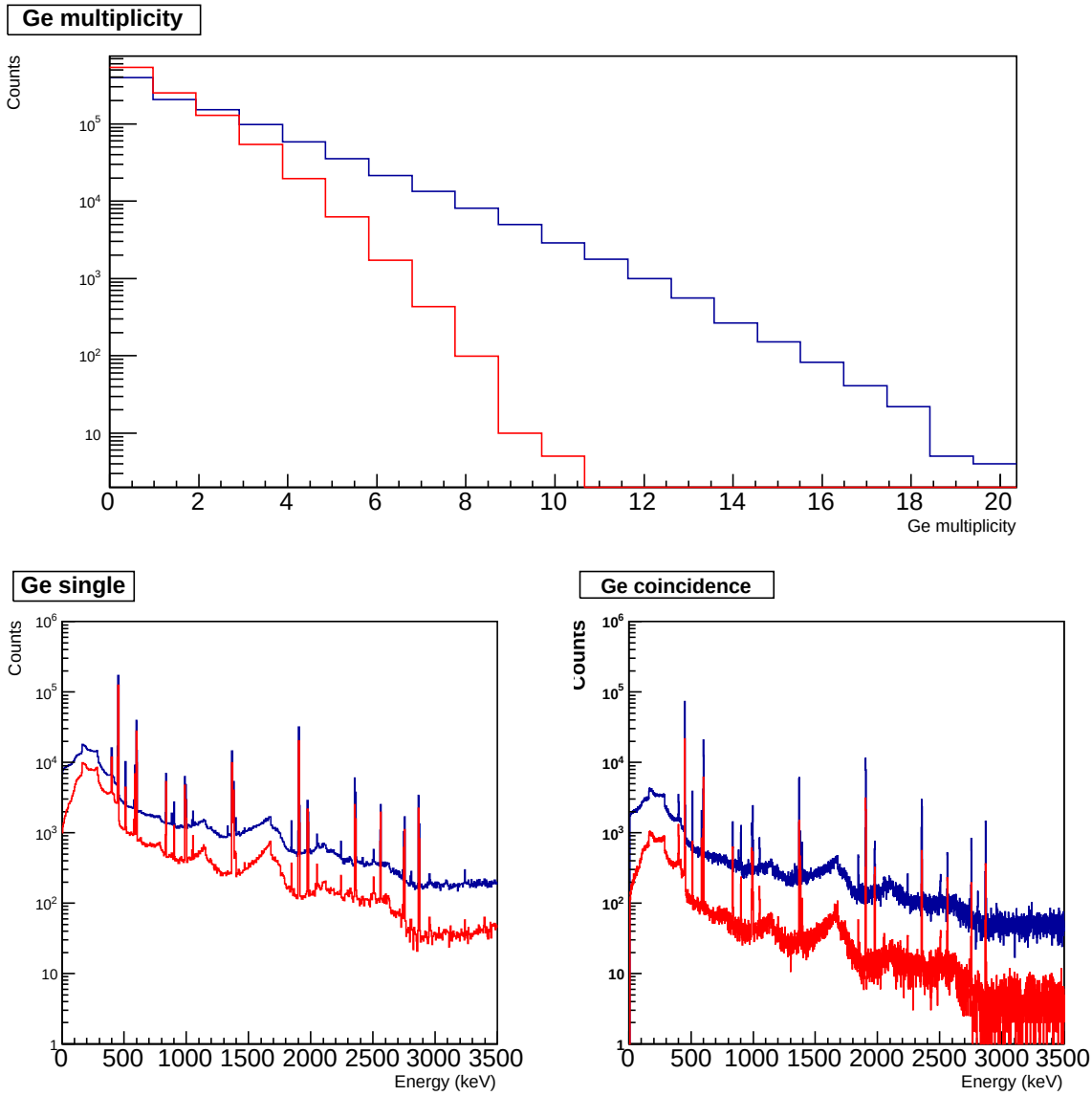

FIG. 7: Results of the simulation with the Geant4 package. In all plots, black and red lines are results of a simulation without or with a Compton suppression, respectively. Add-backed events are also included. (Top) a Ge detector multiplicity, (bottom left) energy spectra unfolded into single γ events, (bottom right) energy spectra unfolded into to $\gamma\gamma$ coincidence events. For example, a 3-fold coincidence is unfolded into 3 single γ events and 3 $\gamma\gamma$ events.

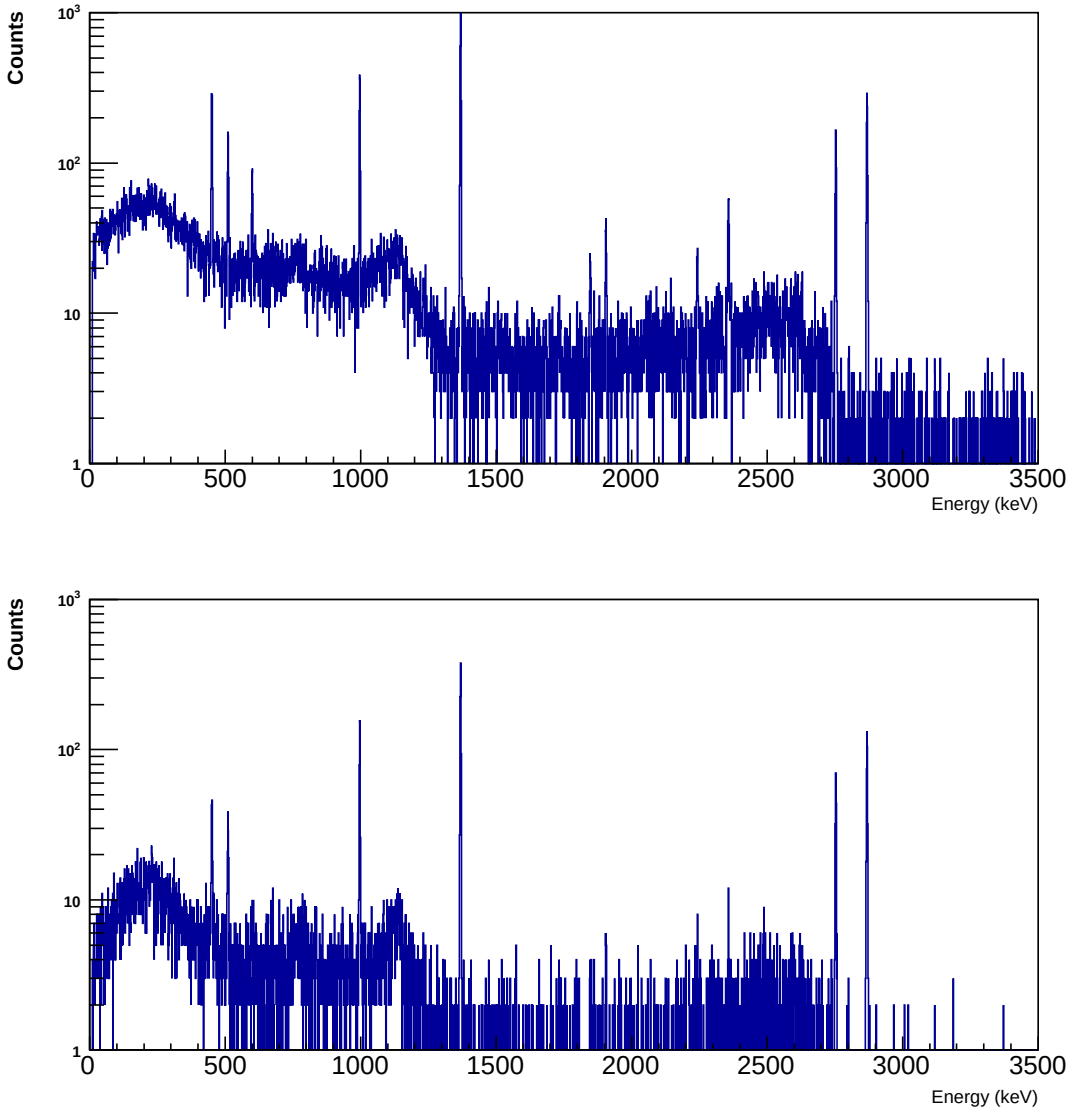

FIG. 8: Spectra obtained by gating on the $E_\gamma(2^+ \rightarrow 0^+;1369\text{keV})$ transition in ^{24}Mg (top) without the Compton event suppression and (bottom) with.